

## FAILURE PROCESS OF ETFE FOILS

DÁNIEL T. KARÁDI\*, DEZSÓ HEGYI\*

\* Department of Mechanics, Materials and Structures; Faculty of Architecture  
Budapest University of Technology and Economics  
Műgyetem rkp. 3., H-1111 Budapest, Hungary  
e-mail: karadi.daniel@epk.bme.hu, web page: <http://www.szt.bme.hu>

**Keywords:** Polymer, ETFE foil; Fracture Mechanics; J-integral.

**Summary.** The present study investigates the failure process of Ethylene tetrafluoroethylene (ETFE) foil on 250  $\mu\text{m}$  thick Novoflon ET 6235Z, a material extensively employed in the building industry. ETFE structures tend to fail due to a rupture in the foil rather than reaching their ultimate stress or strain level in an extended area. Determining the fracture toughness and the level at which unstable crack growth occurs is imperative when considering in-situ material repair. Despite the extensive research conducted on the viscoelastic mechanical behavior of ETFE foils<sup>1-3</sup>, relatively few studies have been found in connection with the fracture mechanical investigation of the foil<sup>4</sup>. ETFE is a ductile polymer film, resulting in a large plastic zone around a crack tip, which highlights the necessity of using methods in elastic-plastic fracture mechanics. Here, the energy release rate, termed J-Integral<sup>5,6</sup> connecting to the crack propagation ( $\Delta a$ ) is investigated based on the work of Hegyi and Pellegrino<sup>7</sup>. Unidirectional tensile tests were conducted on 50mm wide, 300mm long strips with different slit widths (3mm to 18mm) positioned at the center. Three different strain rates (0.083%/s, 0.166%/s, and 0.333 %/s) and three different temperature levels (16°C, 24°C and 32°C) were investigated. The J-integral was calculated around the tip of a crack from the strain field measured by digital image correlation. The critical level of J-integral is determined when the crack starts to propagate. The results show that the value of the critical level of J-integral is independent of the slit width but is proportional to the temperature change. The findings of this study offer significant potential for future research and development in the field of environmentally sustainable structural design, to prolong the service life of the material even in the event of a defect.

### 1 INTRODUCTION

Ethylene tetrafluoroethylene (ETFE) is a thermoplastic semicrystalline polymer used as a thin foil in inflated cushions in the building industry. The structural integrity of these cushions highly depends on their internal pressure. In case of a sharp surface defect, two scenarios are possible. First, after the damage, the crack propagation stops and the air escapes, which drops the level of the internal pressure. The second possibility is if an unstable crack occurs and the structure fails like a balloon. The failure process is highly governed by the ductile behaviour of ETFE as a polymer. First, the sharp crack tip blunts, then a significant plastic zone evolves in the material around the tips. The propagation starts when the stored energy level in the material reaches a critical level<sup>8</sup>. The material parameter called fracture toughness quantifies the resistance of a material to crack initiation under stress. Because of the large plastic zone around the crack tip, Elasto-Plastic Fracture Mechanics (EPFM) approaches should be used to characterise the fracture toughness.

One method is the Essential Work of Fracture (EWF) method<sup>9</sup>. In this approach, the work of the tensile machine is measured while uniaxially loading double-edged notched specimens. The advantage of this method is that the plastic deformation localises into a narrow region between the notches. A drawback is the necessity of numerous measurements, as the measured energy level is related to the ligament length and thickness<sup>10</sup>. Rigotti et al. determined a fracture toughness parameter by the EWF method for ETFE<sup>4</sup>.

Another conventional but standardised method is the determination of the J-integral<sup>5,6</sup>. The J-integral characterises the energy release rate of the crack propagation on a closed path around the crack tip. Traditionally, the J-integral was applied to metals and thick materials. However, Hegyi and Pellegrino<sup>7</sup> conducted measurements on Linear Low-Density Polyethylene (LLDPE) foils, measuring the J-integral level successfully.

In this paper, the J-integral was investigated on rectangular ETFE specimens (NOWOFLON ET 6235) with a slit in the centre. The material was considered a continuum, and the micromechanical behaviour of the cracking process was not investigated. To characterise the fracture toughness of ETFE, the critical level of J-integral ( $J_c$ ) should be determined by investigating the strain field of the specimen around the crack tip. The  $J_c$  was obtained for three different temperature levels (16°C, 24 °C, 32°C) and on three different strain rates (0.083%/s, 0.166%/s, and 0.333 %/s). The effect of different slit lengths was also investigated at 24°C and 0.166%/s test speed.

The second chapter of this paper briefly introduces the J-integral theory and its calculation in the case of ETFE foils. The third chapter details the measurement configurations. The fourth chapter describes the results and discussion, and the paper is finished with a conclusion.

## 2 DETERMINATION OF J-INTEGRAL

Cherepanov<sup>5</sup> and Rice<sup>6</sup> simultaneously developed the J-integral theory. It is a path-independent line integral (Figure 1.), representing the fracture energy per unit crack surface.<sup>11,12</sup>

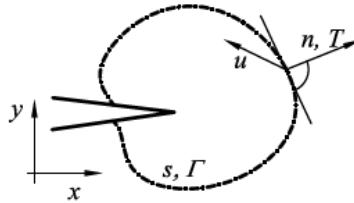


**Figure 1:** Integration path around a crack tip.<sup>7</sup>

The value of J-integral on a closed path  $\Gamma$  around the crack tip is given by:

$$J = \int_{\Gamma} (Wn_1 - T_k \frac{\partial u_k}{\partial x}) ds \quad (1)$$

where  $W$  is the strain energy density,  $n_1 = dy/ds$  is the normal strain in the direction perpendicular to  $\Gamma$ ,  $T$  is the traction vector perpendicular to  $\Gamma$  and is defined as  $T_i = \sigma_{ij}n_j$ ,  $u_i$  is the displacement vector components, and  $ds$  is an infinitesimal element along  $\Gamma$ . Generally, the J-integral is path independent if  $\Gamma$  lies purely in the elastic strain region. However, Shih<sup>13</sup> extended the J-integral to inelastic materials even when the  $\Gamma$  crosses the plastic region around the crack tip. In this case,  $\Gamma$  should lie in a region where no unloading occurs, and the total strain theory of plasticity applies.<sup>12</sup>

The J-integral is calculated along a selected path  $\Gamma$  (Eq. 1), which requires knowledge of the strain energy and stress components. Both parameters can be determined numerically by measuring the strains with a Digital Image Correlation (DIC) system along  $\Gamma$ . An isotropic nonlinear viscoelastic-plastic model extended by the Free Volume Model (FVM) was considered to determine the stresses for the traction vector. The model was developed and investigated on ETFE foils by Karádi and Hegyi<sup>14,15</sup> based on the work of Li et al.<sup>16</sup>.

The J-integral analysis requires a constitutive formulation that predicts stress rather than strain. Therefore, the viscoelastic-plastic model of Karádi and Hegyi<sup>15</sup> was inverted to compute the second Piola-Kirchhoff stresses from the corresponding Green-Lagrange strains (obtained from the DIC) according to the following expression:

$$\sigma_t = (\varepsilon_{t'} + f_{t'-\Delta t'} - \varepsilon_{pl,t-\Delta t} + \Delta\varepsilon_{pl})\tilde{S}_{t'}^{-1} \quad (2)$$

Where  $\tilde{S}_{t'}^{-1}$  is the inverse of the time-dependent isotropic compliance matrix  $\tilde{S}_{t'}$ .  $\varepsilon_{t'}$  is the strain at the current time step,  $f_{t'-\Delta t'}$  is the free-volume-dependent strain increment from the previous time step,  $\varepsilon_{pl,t-\Delta t}$  is plastic strain from the previous step, and  $\Delta\varepsilon_{pl}$  is the plastic strain increment at the current step. Finally, it was assumed that only the elastic strain energy affects the crack propagation, and the dissipated strain energy contributes to the creep and plastic deformation. First, the total strain energy at a given time step  $t$  for a general element of the Prony series  $i$  is given by

$$W_t = \sum_{i=0}^n \varepsilon_i^T \sigma_i \quad (3)$$

Then the dissipated energy density is calculated by

$$W_t^D = W_t - W_t^E, \quad (4)$$

Where  $W_t^E$  is the elastic strain energy density given by

$$W_t^E = \sum_{i=0}^n \varepsilon_i^T \mathbf{E} \varepsilon_i \quad (5)$$

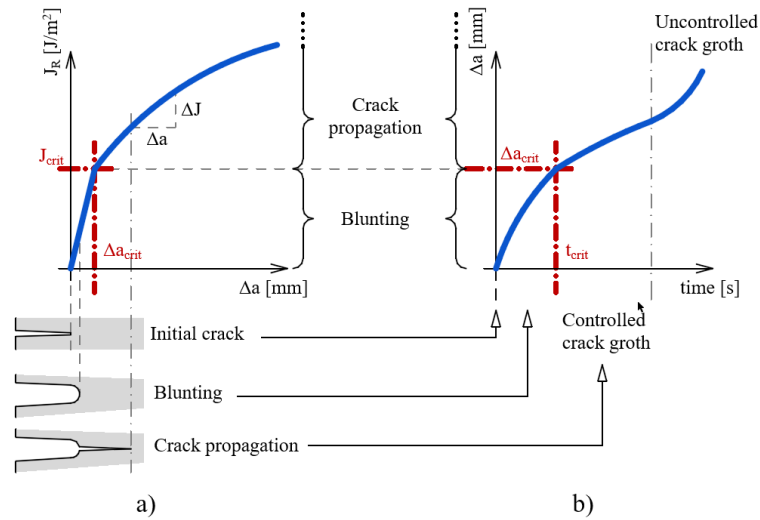


**Figure 2:** a) Schematic diagram of  $J - \Delta a$  curves with blunting phase and crack propagation phase, b) shows the corresponding  $\Delta a - t$  curves with the value of  $\Delta a_{crit}$  marking the end of the blunting phase.

The value of the critical level of J-integral ( $J_c$ ) was given from equation 1 at the time when the crack propagation starts, marked by the critical crack initiation point  $\Delta a_{crit}$  as show in

Figure 2.

## 2 MEASUREMENT CONFIGURATION

The ETFE strip specimens of  $50 \times 300$  mm dimensions were made from NOWOFLON ET 6235<sup>17</sup> foil with printed silver patterns. The nominal thickness was  $250 \mu\text{m}$ , while actual thicknesses, measured with digital callipers, averaged  $245.1 \mu\text{m}$  (standard deviation  $5.03 \mu\text{m}$ ). Testing was conducted with specimens oriented in the machine direction (MD), assuming isotropic behaviour as outlined in Section 1. On each specimen, a slit was made by a sharp scalpel in the centre, perpendicular to the longer direction, to investigate the mode I fracture type.

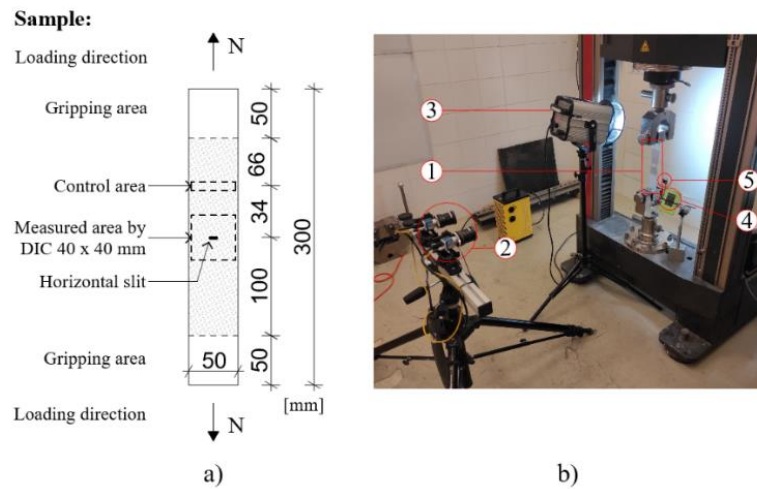


**Figure 3:** Schematics of a) specimen dimensions and configuration and b) machine configurations in the room, (1) test specimen clamped into the material testing machine, (2) DIC camera system, (3) spotlight aimed at the white wall improving lighting conditions, (4) thermometers with (5) thermocouples for temperature and vapour content monitoring.

Two measurement series were conducted based on the slit width. In the first, specimens with a nominal slit length of 6 mm were tested in a tempered room at three temperature levels ( $16 \text{ }^\circ\text{C}$ ,  $24 \text{ }^\circ\text{C}$ , and  $32 \text{ }^\circ\text{C}$ ) and three strain rates ( $0.083\%/s$ ,  $0.166\%/s$ , and  $0.333\%/s$ ), with five specimens per configuration. In the second series, specimens with varying slit widths (3–18 mm in 3 mm increments) were tested at  $24 \text{ }^\circ\text{C}$  and a strain rate of  $0.166\%/s$ , using three specimens per configuration. In total, 75 measurements were performed.

Uniaxial tensile tests were performed until separation in a universal tensile testing machine (ZWICZK Z150) with a waved gripping head (Figure 3). Load measurements were recorded using a 150 kN capacity load cell. A preload of 5 N was applied to prevent wrinkling of specimens.

The strain field was measured using a Digital Image Correlation (DIC) system<sup>18</sup> to capture the in-plane deformation of the ETFE foils. Two Basler acA1920-155um cameras, each equipped with 75 mm Kowa LM75HC F1.8 lenses, recorded the specimens during uniaxial tensile tests. The cameras were about 1.5 m from the specimen, capturing a field of view of roughly  $5 \times 10$  cm. To enable DIC analysis, the silver patterns were removed with acetone first. Then the specimens were coated with a light matte black spray to generate a random speckle pattern.

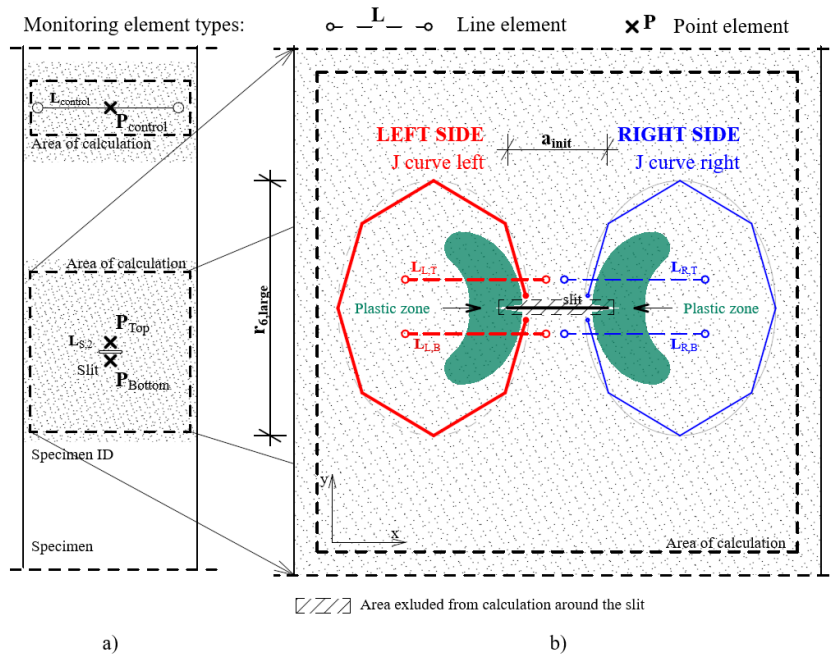


**Figure 4:** The defined monitor lines and points around the crack tip for post-processing the DIC measurements. a) The defined area of calculations with the monitoring points and lines for control. b) Defined monitoring lines and polylines around the crack tips.

Image processing was performed in VIC-3D 8.0<sup>18</sup> with a correlation subset size of  $21 \times 21$  pixels and a step size of 7. During the post-process monitoring to check the validity of the material model monitoring point  $P_{control}$  and line  $L_{control}$  (Figure 4), were used. To investigate the crack fronts' opening along the  $y$  direction monitoring points  $P_{Top}$  and  $P_{Bottom}$  were defined. To measure the crack tip propagation, this study uses the method of Filho et al.<sup>19</sup>, who proposed a method with DIC for crack tip detection of fibrous soft composites. First monitoring lines  $L_{L,T}$ ,  $L_{L,B}$ ;  $L_{R,T}$ ,  $L_{R,B}$  are defined below and above the crack on the two sides. Then, the  $x$  position of the crack tip in the time history could be determined from the average displacement differences between the lines on the same side. To calculate the J-integral to polylines by 9 points, forming elliptical paths around both sides ( $L_1$  and  $R_1$ ) of the crack tips were defined. (Figure 4). The shape of polylines  $L_1$  and  $R_1$  were determined so that it would remain in the elastic range for as long as possible during the measurement. From the post-process, the Green-Lagrange strain tensors were obtained directly from the software.

### 3 RESULTS

#### 3.1 Effect of the initial slit width

First, the mean stress-strain curve was investigated in the control area by examining the influence of plastic deformation on the failure at a temperature level of 24 °C and a speed of 0.167 %/s. The stress level was determined at  $\Delta a_{crit}$  in case of all measurements with a different slit width. The measurements where the slit width was smaller than 9 mm showed that the whole material should yield. In contrast, most of the specimens remained in the elastic phase in the case of measurements with a larger slit width, larger than 9 mm. In these cases, the decrease in ligament length increased local stresses, which enlarged the plastic zone near the advancing

crack tip.

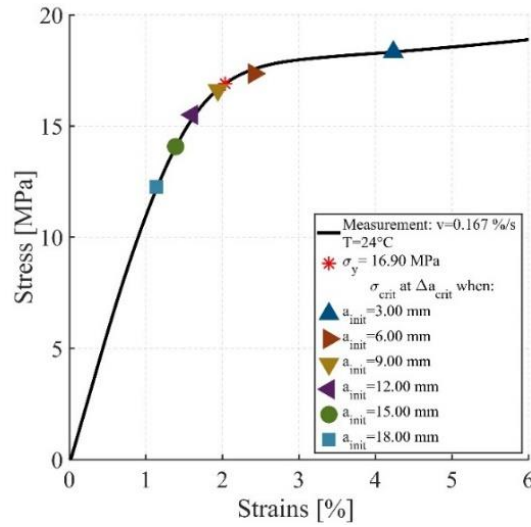


**Figure 5:** The average stress-strain curve of measurement at temperature 24°C and strain rate 0.166  $\frac{\%}{s}$ . The critical stress values  $\sigma_{crit}$  when the crack propagation starts  $\Delta a_{crit}$  for crack widths 3mm to 18mm for the left and right sides of the crack tips were marked by different shapes.

Investigating the values of the critical level of J-integral, in most cases, the stored energy remained mostly around  $9000 \text{ J/m}^2$  (Table 1). One exception was for the 3mm initial slit width, which was considered an outlier in the results. Another outlier seemed to be the measurements with slit widths 15 and 18 mm where above  $10000 \text{ J/m}^2$ .

**Table 1:**  $J_{crit}$  values at  $\Delta a_{crit}$  for different slit width

		$a_0$ [mm]					
		3	6	9	12	15	18
$J_{crit} [\text{J/m}^2]$	Total	12283	12460	10083	10715	11553	11490
	Stored	6664	9012	9230	9396	10292	10370

### 3.2 Effect of the temperature level changes

The temperature dependence of  $J_{crit}$  was investigated at a reference strain rate of 0.166%/s using specimens with an initial crack width of 6 mm, selected to ensure yielding in the whole specimens at crack initiation. To evaluate temperature effects, the mean  $J_{crit}$  values from the left and right integration paths were averaged. As shown in Table 2, all values remained below  $9,000 \text{ J/m}^2$  and decreased with temperature, with the maximum at 16 °C and the minimum at 32 °C.

**Table 2:** shows the mean values of  $J_{crit}$  as a function of temperature at a strain rate 0.166%/s

Temperature /	J-integral [ $J/m^2$ ]	
	Stored	Total
16 °C	8145	10319
24 °C	7973	10864
32 °C	6295	7803

This observation is typical of glassy thermoplastics, which Kinloch and Young<sup>20</sup> detailed. However, the temperature-dependent behavior of polymers is quite complex; further investigations on wider temperature ranges are necessary to map this behavior for ETFE precisely.

### 3.3 Effect of the strain rate changes

As the material model considerably overpredicts or mildly underpredicts the stress-strain response (as shown in Figure 6), the strain rate-dependent behaviour of the critical level of J-integral was treated with caution.

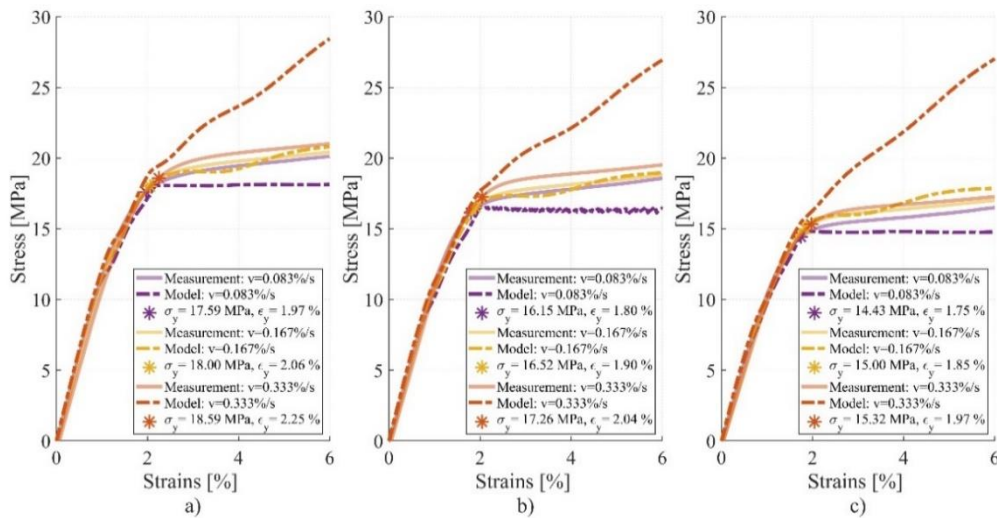


**Figure 6:** Stress-strain control plot for the nonlinear viscoelastic plastic material model on specimens with slit width  $a = 6mm$  at strain rates 0.083 %/s ,0.166 %/s ,0.333 %/s at a) temperature 16 °C b) temperature 24°C c) temperature 32 °C . The plot shows the average values of the five measurements under the same conditions.

Table 3. illustrates this issue with the material model: the fastest loading rates consistently lead to  $J_{crit}$  values that are 1.5 to 2 times higher. In most cases, a higher strain rate corresponded to a higher  $J_{crit}$ .

**Table 3:** shows the mean values of  $J_{crit}$  as a function of temperature at temperature 24°C.

Strain rate /	J-integral [ $J/m^2$ ]	
	Stored	Total
0.083 %/s	5525	11967
0.166 %/s	7956	10860
0.333 %/s	13029	16608

## CONCLUSIONS

This study presents a fracture-mechanical study of ETFE foil (NOWOFLON ET 6235, 250  $\mu\text{m}$ ) using elastic–plastic fracture mechanics based on the J-integral. Centre-notched specimens ( $50 \times 300$  mm) were tested to construct  $J - \Delta a$  resistance curves and determine the critical J-integral,  $J_{crit}$ , under varying temperature and strain rate conditions. Deformations were recorded with a stereo DIC system, while stresses were derived from a nonlinear viscoelastic–plastic model.

Two test series were performed. The first, at 24 °C and 0.166%/s, varied initial slit widths from 3 to 18 mm. The second examined temperature (16, 24, 32 °C) and strain rate effects (0.083, 0.166, 0.333%/s) using 6 mm slits. Crack initiation ( $\Delta a_{crit}$ ) was determined from DIC-based displacement fields using the method of Filho et al.<sup>19</sup>, with bilinear fitting of  $\Delta a - t$  curves marking the transition from blunting to propagation. The mean value of J-integrals was evaluated along an elliptical  $\Gamma$ -path from the left and right side.

At 24 °C and 0.166%/s,  $J_{crit}$  was around 9000 J/m<sup>2</sup>, independent of initial crack width. Increasing temperature reduced  $J_{crit}$  from ~8200 to ~6000 J/m<sup>2</sup>. Strain rate effects were less conclusive due to model limitations, though results were consistent at the reference rate. Tests with different slit widths indicated that cracks shorter than 6 mm did not propagate unstably; for larger slits, parts of the specimen remained elastic, limiting energy release.

Overall, ETFE foils showed low sensitivity to small cracks, as propagation requires the whole section to yield. In inflated cushion systems, internal pressure drops when defects occur, further reducing driving forces for crack growth. Thus, small cracks are unlikely to cause unstable tearing, and repairs by simple on-site patching remain a practical solution.

## ACKNOWLEDGEMENTS

The authors acknowledge support of GRABOPLAN Kft. (9027 Győr, Bútorgyári u. 4.) who provided the ETFE foil for this research.

The DIC system was supported by the European Union and the Hungarian Government in the framework of Competitive Central-Hungary OP (Project ID: VEKOP-2.3.3-15-2017-00017).

## REFERENCES

- [1] Li, Y., M. Wu. “Uniaxial creep property and viscoelastic–plastic modelling of ethylene tetrafluoroethylene (ETFE) foil,” *Mech Time-Depend Mater.* 2015;19(1):21-34. doi:<https://doi.org/10.1007/s11043-014-9248-2>
- [2] Comitti, A., F. Bosi. “Thermomechanical Characterisation and Linear Viscoelastic Modelling of Etfе Foils,” *SSRN*. Preprint posted online June 16, 2023. [https://papers.ssrn.com/sol3/papers.cfm?abstract\\_id=4481374](https://papers.ssrn.com/sol3/papers.cfm?abstract_id=4481374)
- [3] Comitti, A., F. Bosi. “Thermomechanical characterisation and plane stress linear viscoelastic modelling of ethylene-tetra-fluoroethylene foils,” *Mech Time-Depend Mater.* Published online August 28, 2024. doi:10.1007/s11043-024-09704-5
- [4] Rigotti, D., R. Elhajjar, A. Pegoretti. “Adiabatic effects on the temperature and rate dependency of the fracture toughness of an ethylene-fluoroethylene film,” *Engineering Fracture Mechanics.* 2019;214:260-269. doi:<https://doi.org/10.1016/j.engfracmech.2019.03.005>

- [5] Cherepanov, G.P. “Crack propagation in continuous media: PMM vol. 31, no. 3, 1967, pp. 476–488,” *Journal of Applied Mathematics and Mechanics*. 1967;31(3):503-512. doi:10.1016/0021-8928(67)90034-2
- [6] Rice, J.C. “A path-independent integral and the approximate analysis of strain,” *Journal of Applied Mechanics*. 1968;35(2):379-386. doi:https://doi.org/10.1115/1.3601206
- [7] Hegyi, D., S. Pellegrino. “Viscoplastic tearing of polyethylene thin film,” *Mech Time-Depend Mater*. 2015;19(2):187-208. doi:10.1007/s11043-015-9259-7
- [8] Grellmann, W., B. Langer, eds. “*Deformation and Fracture Behaviour of Polymer Materials*,” Vol 247. Springer International Publishing; 2017. doi:10.1007/978-3-319-41879-7
- [9] Chan, W.Y.F., J.G. Williams. “Determination of the fracture toughness of polymeric films by the essential work method,” *Polymer*. 1994;35(8):1666-1672. doi:10.1016/0032-3861(94)90840-0
- [10] Mai, Y.W., B. Cotterell. “On the essential work of ductile fracture in polymers,” *Int J Fract*. 1986;32(2):105-125. doi:10.1007/BF00019787
- [11] Broek, D. “*Elementary Engineering Fracture Mechanics*,” Springer; 1982.
- [12] Gross, D., T. Seelig. “*Fracture Mechanics: With an Introduction to Micromechanics*,” Springer; 2011. doi:10.1007/978-3-642-19240-1
- [13] Shih, C.F. “Relationships between the  $J$ -integral and the crack opening displacement for stationary and extending cracks,” *Journal of the Mechanics and Physics of Solids*. 1981;29(4):305-326. doi:10.1016/0022-5096(81)90003-X
- [14] Karádi, D., D. Hegyi. “Direction Dependent Mechanical Behavior of ETFE Foils,” *Építés - Építészettudomány*. 2025;53(1-2):87-103. doi:10.1556/096.2025.00141
- [15] Karádi, D., D. Hegyi. “Nonlinear thermoviscoelastic modelling of ETFE foils using free volume model,” *Construction and Building Materials*. 2025;482:141578. doi:10.1016/j.conbuildmat.2025.141578
- [16] Li, J., K. Kwok, S. Pellegrino. “Thermoviscoelastic models for polyethylene thin films,” *Mech Time-Depend Mater*. 2016;20(1):13-43. doi:10.1007/s11043-015-9282-8
- [17] NOWOFLON ET Architecture. Accessed January 11, 2025. <https://www.nowofol.com/en/products/nowoflon-et-architecture/>
- [18] Correlated Solutions Digital Image Correlation. Correlated Solutions Digital Image Correlation. 2024. Accessed July 5, 2024. <https://www.correlatedsolutions.com>
- [19] Filho, J., J. Xavier, L. Nunes. “An Alternative Digital Image Correlation-Based Experimental Approach to Estimate Fracture Parameters in Fibrous Soft Materials,” *Materials*. 2022;15(7):2413. doi:10.3390/ma15072413
- [20] Kinloch, A.J., R.J. Young. “*Fracture Behaviour of Polymers*,” Springer Netherlands; 1995. doi:10.1007/978-94-017-1594-2